IL NUOVO CIMENTO Vol. 34 C, N. 5 Suppl. 1 Settembre-Ottobre 2011
DOI 10.1393/ncc/i2011-11009-6

Colloquia: LC10

Minimum bias and soft QCD ATLAS results

R. Di Nardo

Università di Roma "Tor Vergata" and INFN
Via della Ricerca Scientifica 1, 00133 Rome, Italy

(ricevuto il 20 Luglio 2011; pubblicato online il 19 Ottobre 2011)

Summary. — Soft-QCD measurements in proton-proton collisions at $\sqrt{s} = 900\,\text{GeV}$ and $\sqrt{s} = 7\,\text{TeV}$ recorded with the ATLAS detector at the LHC using a single-arm minimum bias trigger are presented. The charged particle multiplicity distribution, its dependence on transverse momentum and pseudorapidity and its correlation with the average transverse momentum will be shown. Moreover, the measurement of the underlying event properties using charged particles is discussed. Finally the measurement of the angular correlations between charged particles is presented. All the measurements are compared with Monte Carlo predictions.

PACS 12.38.Lg – Other nonperturbative calculations.
PACS 12.38.Qk – Experimental tests.
PACS 13.85.Hd – Inelastic scattering: many-particle final states.
PACS 14.40.Df – Strange mesons ($|S| > 0$, $C = B = 0$).

1. – Introduction

The understanding at LHC energies of low-p_T processes in proton-proton collisions is fundamental in order to characterize the underlying event that is an important background for the high-p_T collisions. These soft processes are described by phenomenological models that have to be tuned to the data since perturbative QCD can correctly describe only the hard scattering between partons. Due to the high LHC luminosities, pileup events are unavoidable and they are composed essentially of soft particle production [1, 2] that overlay the interesting hard-scattering events: these can introduce experimental biases in isolation criteria, jet trigger and jet energy scale. It is also important to describe properly the underlying event (UE) that consists of everything except the hard-scattering process in a hadron-hadron collision (the contribution from initial and final state radiation, beam-beam remnants, multi-parton interactions). The charged particle distributions, UE [3,4] and angular correlation [5] measurements performed with the ATLAS experiment [6] at $\sqrt{s} = 900\,\text{GeV}$ and $\sqrt{s} = 7\,\text{TeV}$ in proton-proton collisions are presented.

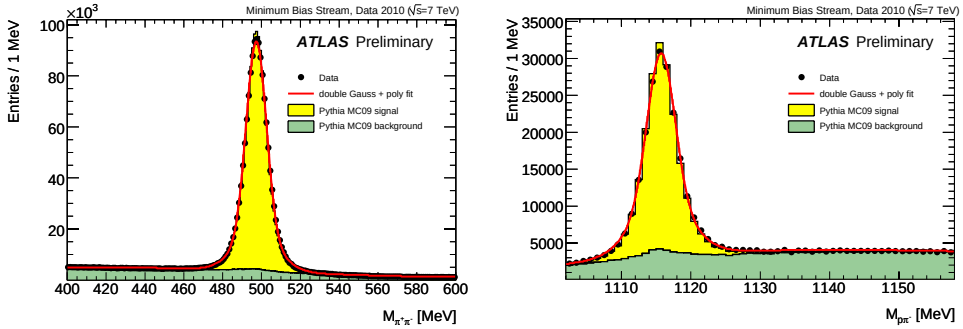

Fig. 1. – K_s^0 (left) and Λ (right) reconstructed mass spectra in proton-proton collision at $\sqrt{s} = 7\,\text{TeV}$ in the barrel region of the ATLAS Inner Detector ($|\eta| < 1.2$ for both tracks) compared with Monte Carlo simulation.

2. – The ATLAS experiment

The ATLAS experiment is one of two general purpose detectors at the Large Hadron Collider. The relevant ATLAS detector components to these measurements include the Inner Detector consisting of three inner subdetectors: the pixel and microstrip subdetectors, which use silicon technology, are complemented with the transition radiation tracker. These detectors allow to reconstruct the tracks of charged particles within $|\eta| < 2.5$. The reconstruction of known particle decays has been used as an important tool to understand the performance of the ATLAS Inner Detector, the track and vertex reconstruction and particle identification capabilities. Figure 1 shows the mass spectra for K_s^0 (left) and Λ (right) reconstructed in the barrel region of the ATLAS Inner Detector ($|\eta| < 1.2$ for both tracks) in proton-proton collision at $\sqrt{s} = 7\,\text{TeV}$. These are compared with Monte Carlo simulation in which signal and background components are separately normalized to data. The agreement demonstrates accuracy of the track momentum scale and excellent modeling of the Inner Detectors 2 T solenoid magnetic field. The Minimum Bias Trigger Scintillator (MBTS [7]) disks are used to trigger in the presence of charged particles in the region $2.09 < |\eta| < 3.84$ and are located on both sides of the detector. The events used in the analyses presented in this paper were triggered requiring the presence of activity on either of the two opposite sides of the MBTS disks.

3. – Charged particle multiplicities

The charged particle multiplicity distributions [1] measured by the ATLAS experiment are

$$(1) \qquad \frac{1}{N_{\text{ev}}}\frac{\mathrm{d}N_{\text{ev}}}{\mathrm{d}n_{\text{ch}}}, \qquad \frac{1}{N_{\text{ev}}}\frac{\mathrm{d}N_{\text{ch}}}{\mathrm{d}\eta}, \qquad \frac{1}{N_{\text{ev}}}\frac{1}{2\pi p_T}\frac{\mathrm{d}^2N_{\text{ch}}}{\mathrm{d}\eta\,\mathrm{d}p_T}, \qquad \langle p_T\rangle \ \textit{vs.}\ n_{\text{ch}},$$

where n_{ch} represent the number of charged particles for a given event, N_{ev} is the number of events with a minimum number of charged particles within the kinematic range selected, N_{ch} is the total number of charged particles in the sample and $\langle p_T\rangle$ is the average transverse momentum for events with a specific value of n_{ch}. Various phase-spaces have been considered for these measurements:

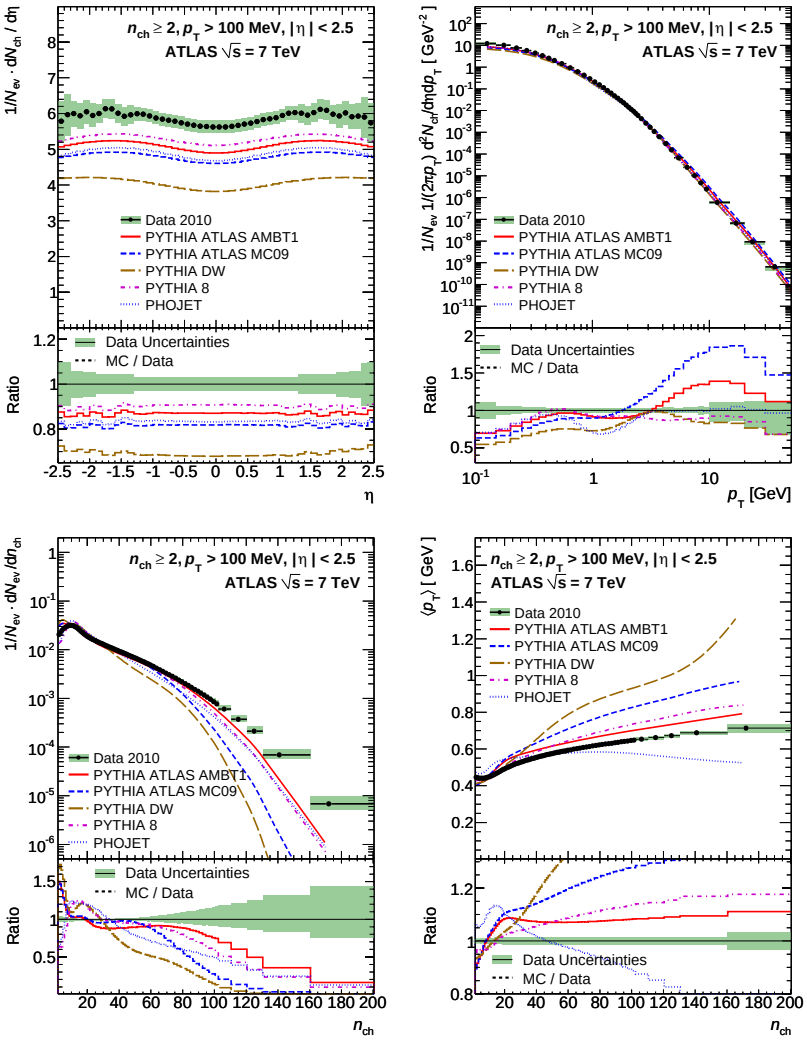

Fig. 2. – The measured charged particle multiplicity *vs.* pseudorapidity (top left), the distribution of the transverse momentum (top right), the multiplicity distribution of charged particles in the event (bottom left) and the average transverse momentum as a function of the number of charged particles (bottom right) compared to different MC predictions.

- $p_T > 0.1\,\text{GeV}$, $n_{\text{ch}} \geq 2$ and $|\eta| < 2.5$ for the most inclusive;
- $p_T > 0.5\,\text{GeV}$, $n_{\text{ch}} \geq 6$ and $|\eta| < 2.5$ for the diffraction suppressed (used to produce the new ATLAS Minimum Bias Tune (AMBT1) [8]);
- $p_T > 0.5\,\text{GeV}$, $n_{\text{ch}} \geq 1$ and $|\eta| < 2.5$, studied also at $\sqrt{s} = 2.76\,\text{TeV}$.

Figure 2 shows the pseudorapidity([1]), p_T, n_{ch} and the average transverse momentum as a function of the number of charged particle distributions measured at $\sqrt{s} = 7\,\text{TeV}$ for the

([1]) Defined as $\eta = -\ln(\tan(\theta/2))$ where θ is the polar angle from the beam axis.

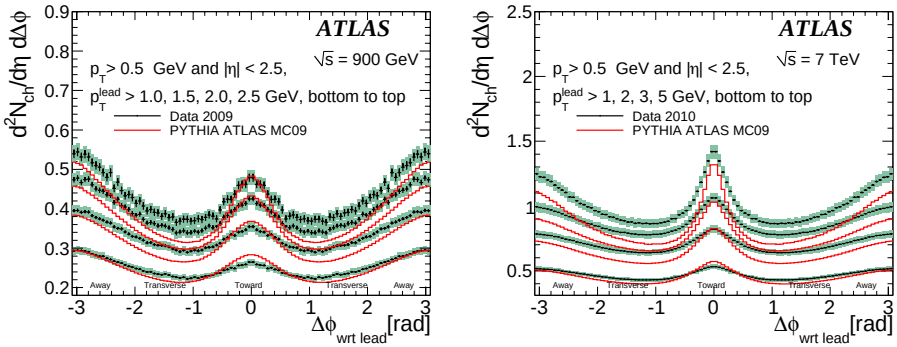

Fig. 3. – $\Delta\phi$ distribution of charged particle densities for $p_T > 0.5\,\text{GeV}$ and $|\eta| < 2.5$ compared to ATLAS Pythia MC09 predictions at $\sqrt{s} = 900\,\text{GeV}$ (left) and $\sqrt{s} = 7\,\text{TeV}$ (right) for different p_T^{lead} thresholds. The error bars show the statistical uncertainty while the shaded areas show the total errors.

phase-space $n_{\text{ch}} \geq 2$, $p_T > 0.1\,\text{GeV}$ and $|\eta| < 2.5$. Data are compared with various MC predictions, including also AMBT1. The shape of the charged multiplicity has a flat shape with a smooth dip in the central pseudorapidity and decreases at forward pseudorapidity. Even if the shape seen in data for $\mathrm{d}N/\mathrm{d}\eta$ is well reproduced in MC predictions, all the models shown underestimate the data. The AMBT1 tune agrees well with the p_T data spectra in the intermediate p_T range between 0.5 and 3 GeV and at high p_T all MC models agree with the data within 20% (with the exception of the ATLAS MC09 tune [9] that reaches 70%) and within 35% at low p_T (with the exception of the PYTHIA DW tune [10] that reaches 45%) where a larger contribution of diffractive events is expected. The charged particle multiplicity distribution per event is not described properly by MC models in the low multiplicity region while AMBT1 agrees within 10% with the data distribution for $n_{\text{ch}} \leq 20$. Finally, the models vary widely in the prediction on the average transverse momentum as a function of the number of charged particles with the AMBT1 that is the closest to the data (agrees within 10%).

4. – Underlying Event studies with charged particles

Although the UE cannot be separated event-by-event from the hard scattering, several observables sensitive to the UE properties can be studied. The $\Delta\phi$ variable, that represents the difference between charged particles and the leading particle azimuthal angle [11], is used to categorized the particles in every event. The region $60^\circ < |\Delta\phi| < 120^\circ$ (transverse region) contains particles from the UE while the regions $|\Delta\phi| < 60^\circ$ (toward region) and $|\Delta\phi| > 120^\circ$ (away region) contains mainly particles from the hard scattering. In order to correct back data to particle level, the same correction for trigger, vertex and tracking efficiency as in the Minimum Bias measurements are applied. Figure 3 shows the $\Delta\phi$ distribution of charged particle densities ($\mathrm{d}^2N/\mathrm{d}\eta\,\mathrm{d}\Delta\phi$) for $p_T > 0.5\,\text{GeV}$ and $|\eta| < 2.5$ for different values of the transverse momentum of the leading particle for data at $\sqrt{s} = 900\,\text{GeV}$ (left) and $\sqrt{s} = 7\,\text{TeV}$ (right). A significant difference in the shape of the $\Delta\phi$ distributions between data and ATLAS Pythia MC09 predictions is seen. With the increase of the leading charged particle p_T, the development of jet-like structure can be observed, as well as the corresponding sharper rise in transverse regions compared to the MC. Figure 4 shows the charged particle density in the transverse region as a

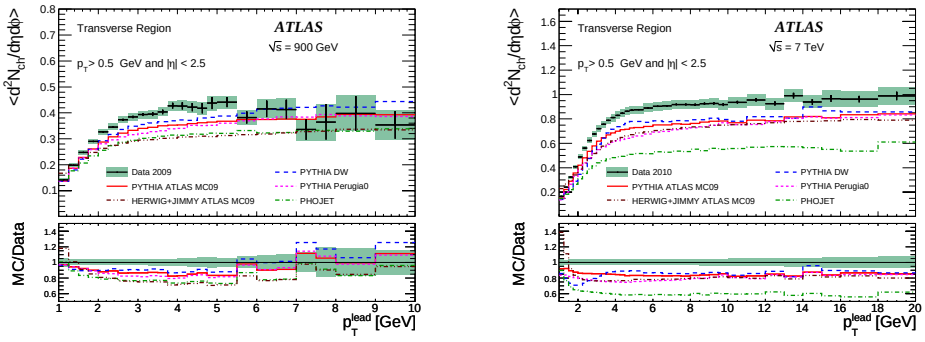

Fig. 4. – Charged particle densities in the transverse region as a function of the p_T of the leading charged particle in p-p collisions at 900 GeV (left) and 7 TeV (right).

function of the p_T of the leading particle for 900 GeV and 7 TeV data. The density rises up to 4–6 GeV due to the increasing probability to have one hard collision and reaches a plateau when the UE activity stops increasing with the transverse momentum of the leading particle. The density value at the plateau is a factor two larger with respect to the multiplicity measured in minimum bias events and this is due to the fact that the high-p_T track selection required for the leading track implies more momentum exchange and a lack of diffractive contribution in the plateau region. Moreover the UE activity is seen to increase by a factor of approximately two between the 900 GeV and 7 TeV data. This is roughly consistent with the rate of increase predicted by MC models tuned to Tevatron data. All the models taken into account show at least 10–15% lower activity in the plateau region with respect to data. The larger difference between data and MC is seen for the PHOJET generator [12] while the PYTHIA DW tune is the closest model to data for the transverse region. Since the JIMMY [13] model requires at least one hard scattering, the strong deviation of HERWIG+JIMMY from the data for low-$p_T^{\rm lead}$ is expected because it is not applicable in this region. An UE analysis has also been performed by the ATLAS experiment using calorimetric information [4]. This incorporates the results obtained by the track based analysis and is also sensitive to the neutral component.

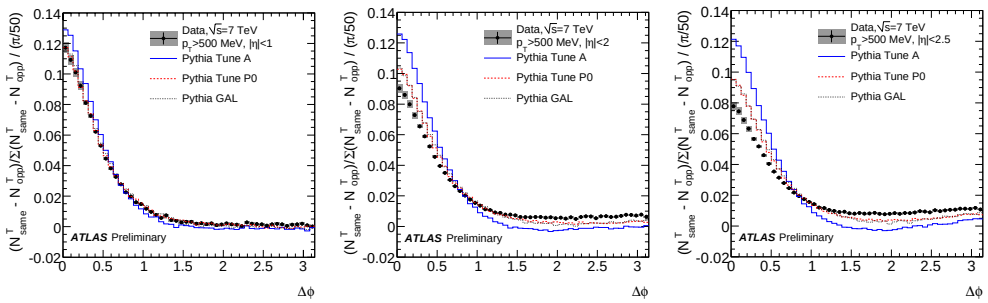

Fig. 5. – The "same minus opposite" distribution for $\sqrt{s} = 7$ TeV for $|\eta| < 1.0$ (left), $|\eta| < 2.0$ (center) and $|\eta| < 2.5$ (right).

5. – Angular correlations between charged particles

The study of angular correlation in toward and away-side regions with respect to the leading particle can be used for further understanding of soft QCD processes since different models provide significantly different predictions of the width and height of the toward and away-side peaks of the $\Delta\phi$ (angles difference in the transverse plane between the leading particle and all the other particles) distribution, making the characteristics of these peaks (*i.e.* width and height) an interesting object of study. In particular the following two distributions have been studied:

- the $\Delta\phi$ *crest shape*, that is obtained from the $\Delta\phi$ distribution subtracting the minimum of the distribution (obtained with a second-order ploynomial fit);
- the $\Delta\phi$ "*same minus opposite*" observable, obtained subtracting the opposite side distribution (defined according to if pseudorapidity has the same sign or the opposite sign as the leading track) from the same side distribution and normalizing to unity.

Figure 5 shows the "same minus opposite" distribution for $\sqrt{s} = 7\,\text{TeV}$ for different η regions. The data (black dots) are compared to the predictions of Pythia tune: tune A [14], tune Perugia0 [15] and GAL [16]. All models describe the distributions poorly, with a better agreement only if the central region is selected ($|\eta| < 1$). These variables can be used as further input for MC tuning.

6. – Conclusions

Charged particle distributions, underlying event distributions and charged particle correlations in p-p collisions at 900 GeV and 7 TeV measured by the ATLAS detector at LHC have been studied. Since most of the pre-LHC models do not show a satisfactory agreement with data, these measurements represent important inputs for MC tuning purposes. In particular, the new AMBT1 tune represents the first improvement for the description of minimum bias results.

REFERENCES

[1] The ATLAS Collaboration, *New J. Phys.*, **13** (2011) 053033, arXiv:1012.5104v2.
[2] The ATLAS Collaboration, *Phys. Lett. B*, **688** (2010) 21, arXiv:1003.3124v2.
[3] The ATLAS Collaboration, *Phys. Rev. D*, **83** (2011) 112001, arXiv:1012.0791v2.
[4] The ATLAS Collaboration, *EPJC*, **71** (2011) 1636.
[5] The ATLAS Collaboration, *Angular correlations between charged particles from proton-proton collisions at* $\sqrt{s} = 900\,\text{GeV}$ *and* $\sqrt{s} = 7\,\text{TeV}$ *measured with ATLAS detector*, ATLAS-CONF-2010-08.
[6] The ATLAS Collaboration, *JINST*, **3** (2008) S08003.
[7] The ATLAS Collaboration, *Performance of the Minimum Bias Trigger in p-p Collisions at* $\sqrt{s} = 7\,\text{TeV}$, ATL-CONF-2010-068.
[8] The ATLAS Collaboration, *Charged particle multiplicities in pp interactions at* $\sqrt{s} = 0.9$ *and* $7\,\text{TeV}$ *in a diffractive limited phase-space measured with the ATLAS detector at the LHC and new PYTHIA6 tune*, ATLAS-CONF-2010-031.
[9] The ATLAS Collaboration, *ATLAS Monte Carlo tunes for MC09*, ATL-PHYS-PUB-2010-002.
[10] Albrow M. G. *et al.*, *Tevatron-for-LHC Report of the QCD Working Group*, arXiv:hep-ph/0610012.

[11] The CDF Collaboration, *Phys. Rev. D*, **70** (2004) 072002.
[12] Engel R., *Z. Phys. C*, **66** (1995) 203.
[13] Butterworth J. M., Forshaw J. R. and Seymour M. H., *Z. Phys. C*, **72** (1996) 637.
[14] Field R. D., *The underlying event in hard scattering processes*, arXiv:hep-ph/0201192.
[15] Skands P. Z., *The Perugia Tunes*, arXiv:0905.3418.
[16] Rathsman J., *Phys. Lett. B*, **452** (1999) 364.